Journal of Visualization, Vol. 5, No. 4 (2002) 335-342

Particle Image Analysis of Open-channel Flow at a Backward Facing Step Having a Trench

Fujita, I.*

* Research Center for Urban Safety and Security, Kobe University, Rokkodai, Nada-ku, Kobe 657-8501, Japan.

Received 24 July 2001.
Revised 30 April 2002.

***Abstract*:** Characteristics of open-channel flow at a backward facing step with a trench section were experimentally investigated. The experiments were performed using a straight open channel flume by varying the trench length. Two-dimensional velocity measurements by the particle tracking velocimetry (PTV) were conducted at the trench section using a high-resolution video camera of 12 fps. Mean and turbulent flow properties along with the water surface profile were measured for various aspect ratios of the trench. It was also observed that the flow at the trench begins to oscillate periodically for a specific aspect ratio of the trench.

***Keywords*:** PTV, backward facing step, trench, hydraulic jump, hydraulic oscillation.

1. Introduction

It is well known that the flow at a backward facing step exhibits complex flow features such as flow separation, development of free shear layer, reattachment of separated flow and a recirculating flow associated with them. Since the flow includes these significant flow features, and in addition, the flow configuration is rather simple, experimental data of the flow (e.g., Itoh and Kasagi, 1989, Nezu and Nakagawa, 1989 and Grant et al., 1992) has been widely used for examining the numerical accuracy of turbulent simulation models (e.g., Arnal and Friedrich, 1993). However, in the case of an open-channel backstep flow, free water surface is easily deformed depending on the tail water condition, which is a considerably different feature from those flows for a closed channel or a boundary layer. When the tail water depth is relatively large the water surface becomes almost horizontal, whereas, when we lower the tail water depth, the free water surface is subject to a large deformation sometimes even accompanying a hydraulic jump.

The flow pattern would become much more complicated when we install a trench section just downstream of the backward facing step; the channel becomes a combination of backward and forward facing steps with different step heights. From the river engineering point of view, this flow configuration is analogous to the flow at a falling work having a trench section just downstream of it. Some examples of such river structure can be found in the Sumiyoshi River in Kobe City. The purpose of this supplementary structure is to provide people a water surface area within the trench (or a small waterfront environment), since in such urban area the normal flow rate is relatively small and the flow environment does not attract people to the river region. However, the flow features associated with this kind of flow have not been investigated so far, although open-channel flows with a trench or a cavity have been investigated by many researchers (e.g., Fujita, et al., 1993 and Nezu et al., 1989). In this paper, experiments using an image analysis method were conducted to examine the effects of the trench aspect ratio to the flow features such as water-surface pattern and turbulence structures.

2. Experiments

2.1 Hydraulic Conditions

The experiments were conducted using a 7.5 m-length open-channel flume with a width of 30 cm. The trench section was set up in the middle of an inclined flume with a bottom slope of 1/500. Schematic of flow parameters at the trench section is shown in Fig. 1. A free falling condition was given at the downstream end of the channel, thus the flow condition changes from subcritical to supercritical at the trench section for the channel configuration shown in Fig. 1. The hydraulic condition is shown in Table 1. The length of the trench was varied between 0.0 cm and 11.0 cm for the same inflow condition. The aspect ratio of the trench a is defined here as $a = L/D$, where L is the length of the trench and D is the relative height of the channel bottoms.

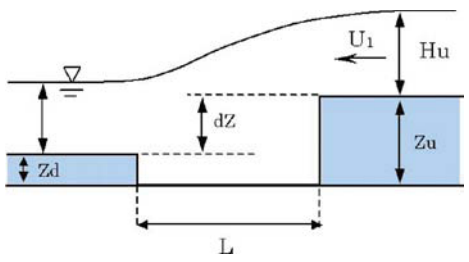

Fig. 1. Schematic of flow parameters.

Table 1. Hydraulic condition.

Discharge Q (m^3/s)	0.00227
Re	7590
Fr_1	0.889
D (cm)	1.0
Zu (cm)	2.0
U_1 (cm/s)	38.9
L (cm)	0.0 -11.0

2.2 Image Analysis System

The image analysis system in the present research is shown in Fig. 2. Images visualized by a laser-light sheet are captured by a high-resolution video camera (Hitachi, KP-F100) with the image-sampling rate of 12 fps (frame per second). The captured image size is 1304 × 1024 pixels with eight-bit resolution. In the present system, 162 consecutive images can be stored on a frame memory installed on a personal computer at one time. A total of 972 (= 162 × 6) images (for about 81 seconds) were used for the image analysis of steady flow conditions. To visualize flow, the flow was seeded by crashed nylon particles with a mean diameter of 60 μm and a specific gravity of 1.02. In the PTV measurement, continuous laser light is chopped by an AOM (Acoustic Optical Modulator) in order to freeze the particle movements within a short time interval. The pulse interval was set at 0.002 seconds, so that the maximum tracer movement becomes less than about ten pixels. The binarized cross-correlation method proposed by Uemura et al. (1989) was used as a PTV algorithm and several hundreds of randomly distributed velocity vectors were obtained from a pair of instantaneous particle images. To minimize the production of erroneous vectors, the area outside of the water region was masked for the cases where the free surface maintains its shape with time. Mean flow properties were calculated from the accumulated data picked up from a small flat mesh,

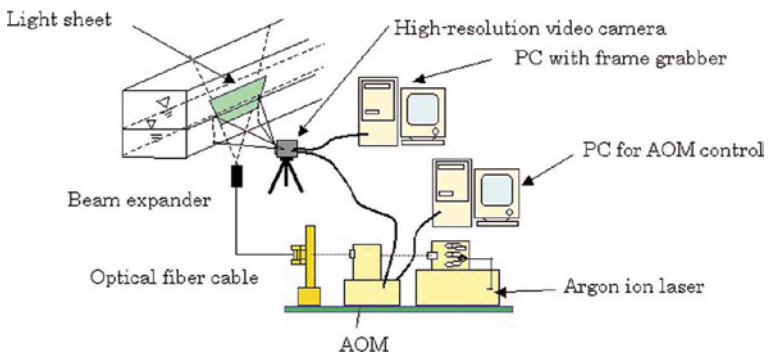

Fig. 2. Image analysis system.

2.5 mm by 1.0 mm, assuming the uniformity of the local flow field within the mesh. The turbulent properties were obtained from velocity values interpolated on the same mesh, since the number of data for each mesh was statistically not enough especially in the highly shearing zone. The total amount of processed image data was about 19 GB (14580 images).

2.3 General Flow Feature

Before conducting detailed PTV measurements, general flow pattern was observed by gradually changing the aspect ratio of the trench or the length of the trench. In the course of this preliminary experiment, it was observed that when the aspect ratio is small ($a < 6.0$ in the present case), the upstream main flow is smoothly connected to the flow in the downstream section without any appreciable water surface fluctuation. On the other hand, as the aspect ratio is increased ($a > 6.0$), the water surface suddenly begins to show quite a periodic oscillation accompanying an breaking of a hydraulic jump, which is an intriguing oscillating flow feature rarely observed in the straight open-channel flow. When we further increase the aspect ratio ($a > 9.5$), the oscillation phenomena cease to occur; instead, a steady hydraulic jump was produced within the trench section. Hence, in the following discussions, steady (non-oscillatory) and unsteady (oscillatory) flow features will be treated separately.

3. Results and Discussions

3.1 Flow Features for Non-oscillatory Conditions

3.1.1 Mean velocity field

Mean velocity vectors (U, V) for the non-oscillatory flow conditions a, less than 6.0 or greater than 9.5, are plotted in Fig. 3. It is shown that mean velocity fields are clearly obtained by the present PTV system. For the range of a less than 3.5, the flow within the trench exhibits a cavity-like flow feature accompanied by a large recirculating vortex with its center near the end of the trench. The main flow seems to have no appreciable interaction with the downstream (forward facing) step since there is no noticeable change in the direction of main stream vectors at the downstream trench section. At $a = 5.5$, however, lower part of the main flow begins to collide with the downstream step, where velocity vectors have small upward components. It should be noted that a small depression of the water surface is present near the end of the trench. For a little larger aspect ratio ($a = 6.0$), the direction of the main stream is completely deflected by the presence of the end wall of the trench, with a new large separation zone on the downstream step. As mentioned previously, when the aspect ratio increases to more than 6.0, the downstream wave suddenly becomes unstable and begins to oscillate periodically. This unstable (oscillatory) mode continues until $a = 9.5$.

When the aspect ratio increases to more than 9.5, the oscillating flow pattern ceases to occur and stable flow patterns are reproduced again as shown in Figs. 3 (e) and (f). In this case, the width of the main stream diverges due to turbulent diffusion, with its direction deflected upward by the downstream vertical wall of the trench. In addition, a stable roller (a steady hydraulic jump) is generated upon the main flow, i.e., the main stream is submerged under the roller with a jet-like vertical velocity distribution in the downstream sections within the trench.

3.1.2 Turbulent properties

Turbulent kinetic energy distributions k for various aspect ratios are shown in Fig. 4. The value of k is calculated from $k = (u'^2 + 2v'^2)/2$ as a first approximation, where u' and v' are the turbulent intensities in the streamwise and transverse components, respectively. For the case of the smaller aspect ratio ($a = 3.5$), the shear layer between the main flow and the cavity area, within which large turbulent kinetic energy is produced, smoothly touches upon the lower step and dissipate in the downstream direction, while for a larger aspect ratio ($a = 5.5$), collision of the lower part of the main flow to the rearward vertical face generates larger turbulent kinetic energy. When the aspect ratio becomes 6.0, in addition to the turbulent properties similar to that for $a = 5.5$, considerably large amount of turbulence is generated within the newly separated shear layer produced at the end of the trench. Finally, in the case of $a = 9.5$, after the oscillation phase, an extremely large turbulent kinetic energy zone is generated along the boundary between the submerged main stream and the roller above the main flow. It is interesting to note that two parallel shear layers are present within the trench section. Figure 5 indicates the distributions of the Reynolds shear stress. It is apparent that regions with large Reynolds stress correspond well with those with large turbulent kinetic energy shown in Fig. 4.

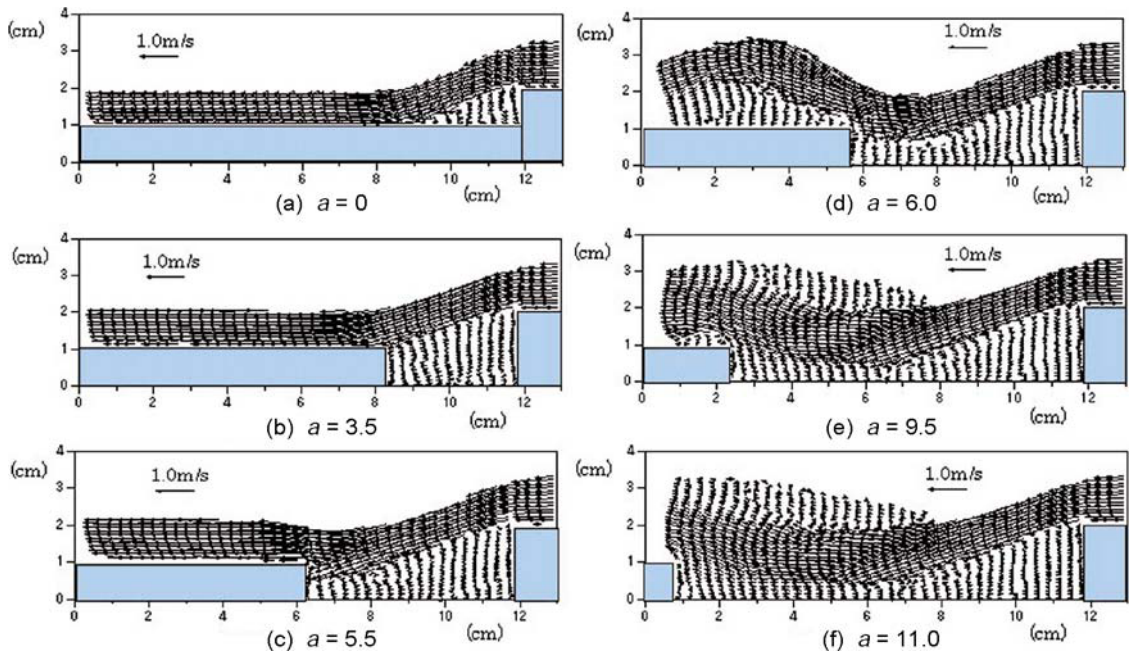

Fig. 3. Mean velocity vectors obtained by PTV for stable cases.

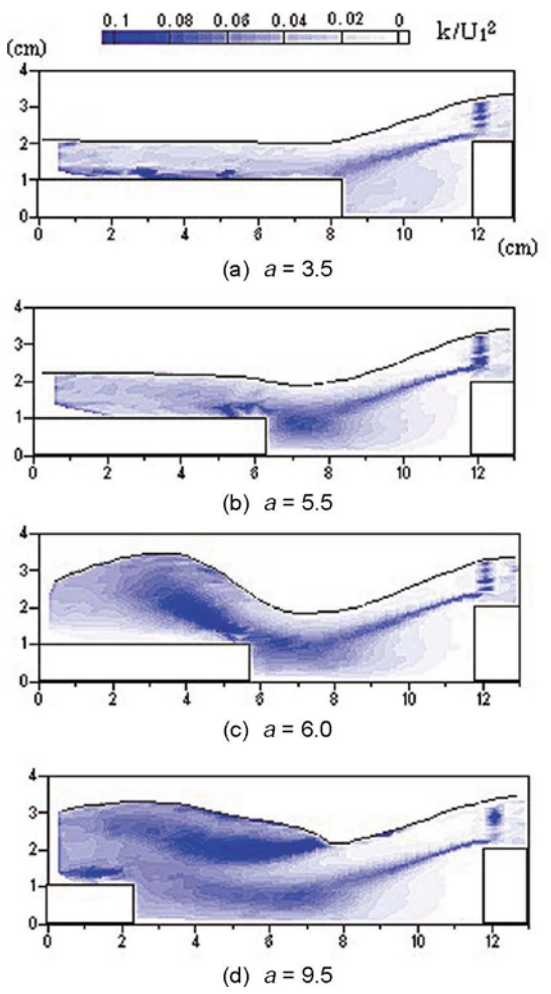

Fig. 4. Distribution of turbulent kinetic energy (non-oscillatory flow).

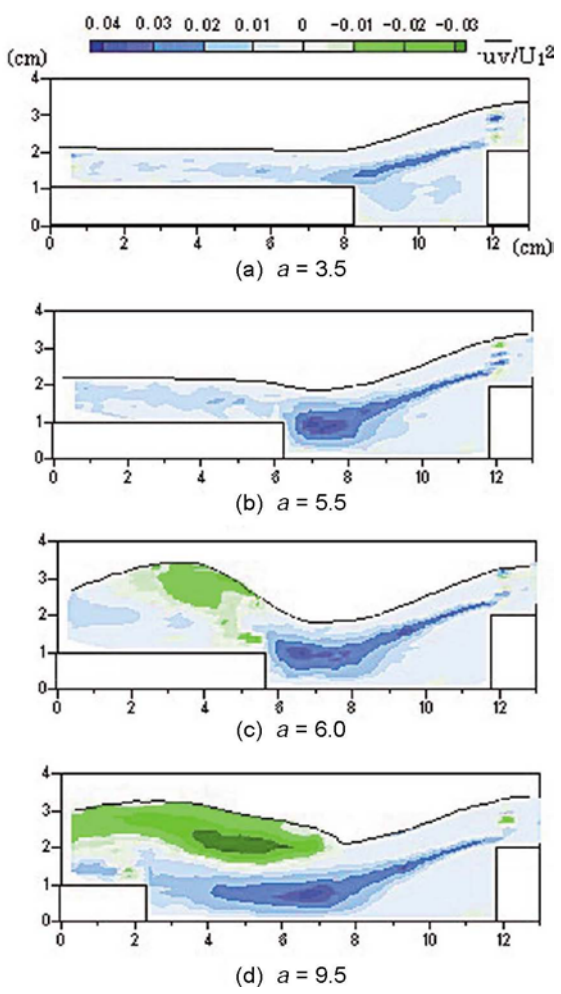

Fig. 5. Distribution of the Reynolds stress (non-oscillatory flow).

3.2 Flow Features for Oscillatory Conditions

For a better understanding of the oscillating flow features, several consecutive images visualized by a continuous laser light sheet are demonstrated in Fig. 6. The images were taken without applying AOM control in order to visualize the particle pathlines with a longer shutter speed. Both large-scale structures in the trench section and surface deformation patterns are clearly visualized. Figs. 6(e)-(g) indicate that the white cap created by the breaking of a hydraulic jump is quickly flashed away by the strong inflow.

Several velocity vector fields during one period of oscillation, about 1.5 seconds in the present case, are shown in Fig. 7. In this figure, randomly distributed velocity vectors are interpolated on the same mesh as the one used in Fig. 3. Erroneous vectors are removed by a statistical treatment and several calculated vectors outside the flow region are removed by referring them to the respective particle images. It is clearly seen from Fig. 7 that very large deformation of water surface is generated for this aspect ratio (a = 6.5). It should be noted that the highest water level produced by the hydraulic jump, found in Fig. 7(c), goes beyond the upstream water level and at the same time the separation zone on the downstream step becomes a maximum. This condition is considerably unstable and the separation zone soon disappears as shown in Fig. 7(d). At the subsequent moment (Fig. 7 (e)), the water depth in the trench section increases due to the continuous supply of mass flux from upstream; as a result, the water surface becomes almost horizontal again with a large recirculating flow within the trench section. To demonstrate the periodic feature of the oscillating phenomenon, evolution of streamwise and vertical velocity distributions in a vertical cross-section in the center of the trench section were reproduced as a spatiotemporal image as shown in Fig. 8. This figure shows that the oscillation phenomenon is quite periodic within the trench section whose influence goes deep into the bottom region both in streamwise and vertical directions.

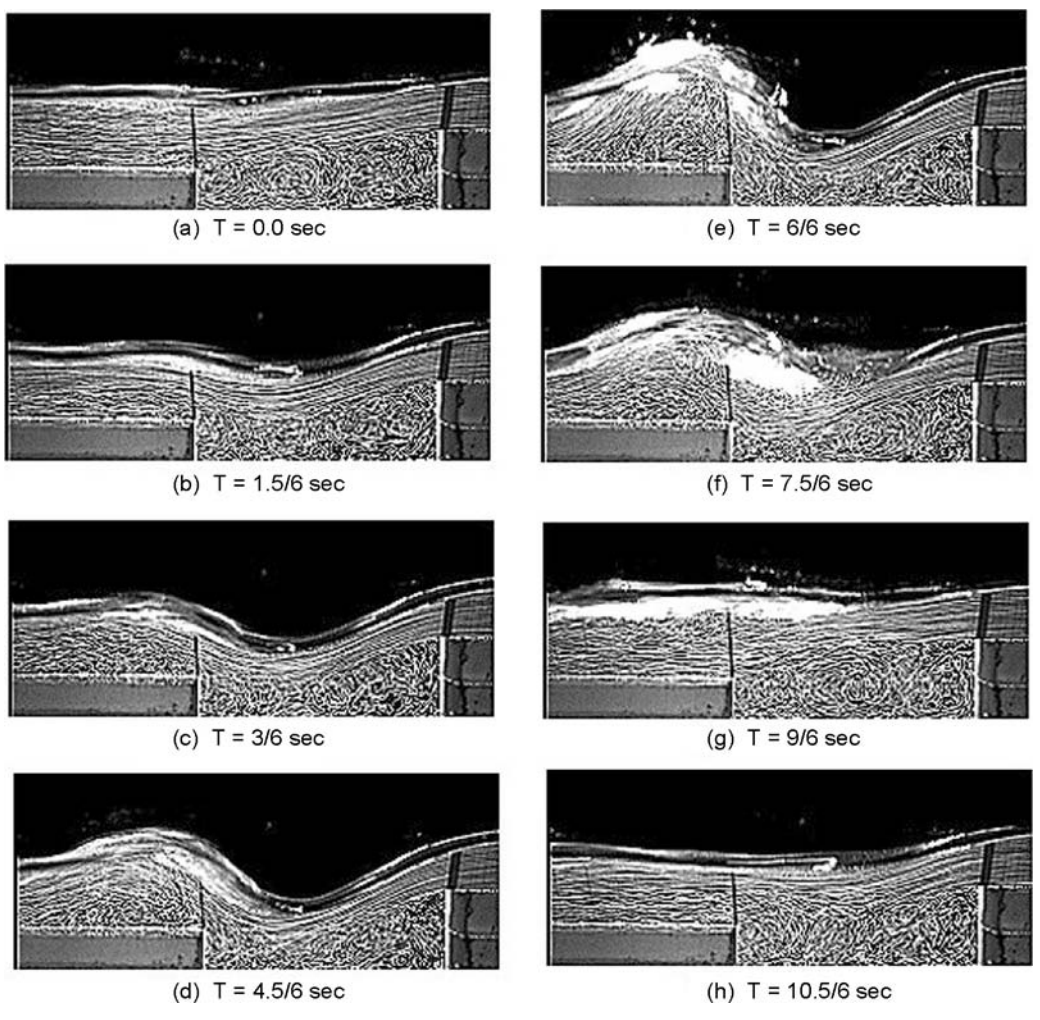

Fig. 6. Consecutive images of oscillating flow (a = 6.5).

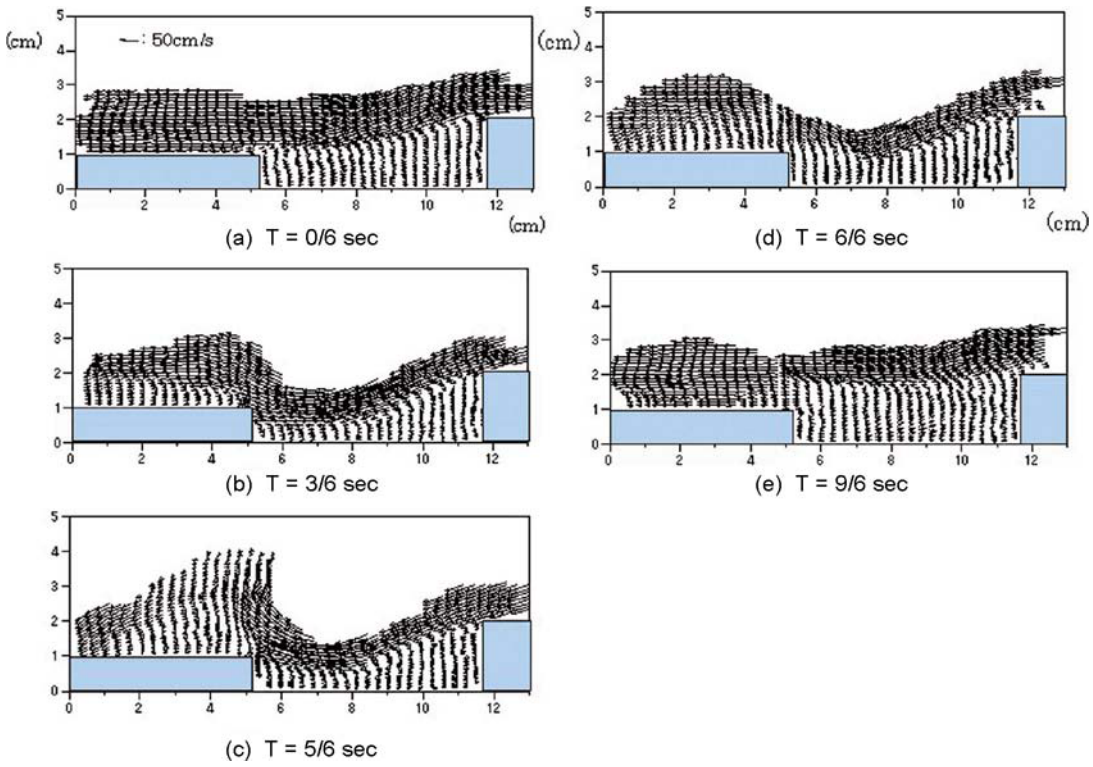

Fig. 7. Instantaneous velocity vectors for one period.

Fig. 8. Time evolution of streamwise and vertical velocity distributions in a vertical cross section in the center of the trench for the case of a = 6.5.

3.3 Mechanism of Oscillation

Figure 9 illustrates the flow pattern in the critical situation or in the neutrally stable condition just before the oscillation begins. In this situation, the flow deflected by the downstream step should balance the celerity of the wave generated on the downstream side of the trench section; namely, streamwise component of the mean velocity at the downstream trench section U_d, should become almost the same as the wave celerity calculated from $c = (gH_{max})^{1/2}$, where H_{max} denotes the maximum wave height in the critical condition and g is the gravitational acceleration. As an example, pay attention to the flow situation shown in Fig. 3(d), which is close to this critical situation. In this case, U_d is about 51 cm/s while c is about 49.5 cm/s using the observed maximum wave height 2.5 cm. Since the wave celerity is a little less than U_d, the created wave is incapable of moving upstream against the mean flow. The most important phenomenon for the oscillation to occur is the creation of a separation zone downstream of the trench that locally raises the water level forming a standing wave as illustrated in Fig. 9. When the size of the separation zone becomes large due to a strong deflection of the main flow, the celerity becomes larger than U_d and the standing wave begins to propagate upstream and finally it breaks down within the trench section. This wave breaking induces an unstable hydraulic jump and the sequence of flow oscillation is initiated.

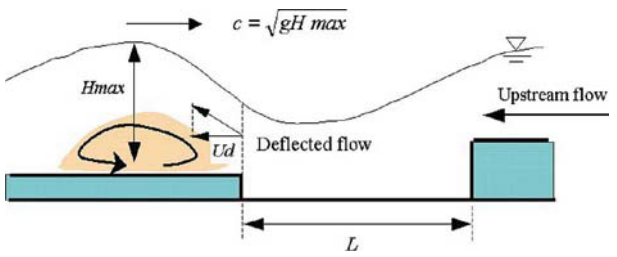

Fig. 9. Schematic illustration of the balance between wave celerity and deflected flow.

4. Conclusion

Spatially varied open-channel flows at a backward facing step with a trench were experimentally investigated by an image analysis method. It was shown that two-dimensional variation of mean and turbulent flow structures can be measured by the present PTV system fairly well. The remarkable feature of the flow is that the surface flow patterns demonstrate a catastrophic change within a narrow range of the trench aspect ratio, accompanied by a periodic oscillation of a hydraulic jump. It was shown that a separation zone created just downstream of the trench due to the main flow deflection is most responsible for the oscillation phenomenon to occur. However, the general relationship between the trench aspect ratio and the oscillation frequency is not clear at present, which has to be clarified in a further study.

Acknowledgment

Cooperation from T. Maruyama, a graduate student from Kobe University, is highly appreciated. This research was financially supported by the Grant-in-Aid for Scientific Research from the Japan Ministry of Education (Project No.12650514, Project leader: Ichiro Fujita)

References

Arnal, M. and Friedrich, R., Large-eddy Simulation of Turbulent Flow with Separation, Turbulent Shear Flows, (1993), 169, Springer-Verlag.

Fujita, I., Kanda, T. and Komura, S., Measurements of Turbulent Flow in a Trench Using Image Processing Technique, Proceedings 5th International Symposium on Refined Flow Modeling and Turbulence Measurements, (1993), 309.

Grant, I., Owens, E. and Yan, Y.-Y., Particle Image Velocimetry Measurements of the Separated Flow Behind a Rearward Facing Step, Experiments in Fluids, 12 (1992), 238.

Itoh, N. and Kasagi, N., Turbulent Measurement in a Separated and Reattaching Flow Over a Backward-facing Step with the Three-dimensional Particle Tracking Velocimeter, Journal of the Flow Visualization Society of Japan, 9-34 (1989), 87. (in Japanese)

Nezu, I. and Nakagawa, H., Turbulent Structure of Backward-facing Step Flow and Coherent Vortex Shedding from Reattachment in Open Channel Flows, Turbulent Shear Flows, 6 (1989), 313, Springer-Verlag.

Nezu, I., Yamamoto, Y. and Onitsuka, K., Numerical Simulation on Turbulent Structures in Cavity Flows by Means of Large Eddy Simulation, Annual Journal of Hydraulic Engineering, JSCE, (1989) 637. (in Japanese)

Uemura, T., Yamamoto, F. and Ohmi, K., A High-speed Algorithm of Image Analysis for Real Time Measurement of a Two-dimensional Velocity Distribution, Flow Visualization, ASME, FED-85 (1989), 129.

Author Profile

Ichiro Fujita : He received his M.Sc. (Eng) degree in Civil Engineering in 1979 and Ph.D. degree in 1990 from Kobe University. He worked in Gifu University from 1982 to 1999. He was a visiting associate professor in the Iowa Institute of Hydraulic Research, the University of Iowa from 1995 to 1996. He has been working as an associate professor in the Research Center for Urban Safety and Security, Kobe University since 1999. His research interests are image measurement of river flow, open-channel turbulence and numerical simulation of rapidly varying flow.